Thermal Analysis, Optimisation and Design of a Martian Oxygen Production Plant

Venkatesh A. Iyer and K.R. Sridhar
Department of Aerospace and Mechanical Engineering
The University of Arizona

Abstract

The objective of this work is to optimally design the thermal components of a system that uses carbon dioxide (CO_2) from the Martian atmosphere to produce oxygen (O_2) for spacecraft propulsion and/or life-support. CO_2 is thermally decomposed into carbon monoxide (CO) and O_2 followed by the electrochemical separation of O_2. The design of the overall system and its various individual components depends on, among other things, the fraction of the stoichiometric yield of O_2 that can be realised in the system and the temperature of operation of the electrochemical separation membrane. The analysis performed indicates that a substantial reduction could be obtained in the mass and power requirements of the system if the unreacted CO_2 were to be recycled. The report also discusses the concepts of an optimum temperature of the Zirconia cell and impracticality of plant operation at low cell efficiencies. The design of the thermal equipment would be such that the mass and power requirements of the individual components and of the overall system would be optimised.

Introduction

There has been tremendous interest in recent years on the need for in-situ-propellant-processing (ISPP) [1,2]. More than 80% of a spacecraft's mass is due to the propellant. Hence production of propellants at locations remote from the Earth is essential for frequent and extended space explorations. Here, the production of Oxygen from the predominantly CO_2 atmosphere of Mars is explored. The system that would be used on Mars would have a filter at the CO_2 intake end to remove the dust and particulates from the supply gas. It would also have a liquefaction and storage unit at the O_2 production end. These components are not being designed by UA/NASA

SERC presently. However, they will be part of our future investigations. The system currently being designed incorporates the sub-systems necessary for supplying the CO_2 at Martian pressures and temperatures. This system will be designed, fabricated and tested extensively on our ground-based facilities. To distinguish it from the future flight-tested system for Mars, the ground-based testing system will be referred to as the "Test Bed".

Description of the Test Bed

The Test Bed, shown in figure 1, can roughly be divided into 4 sub-systems:

1. The simulation sub-system consists of CO_2 supply and a Cryo-Vacuum Chamber cooled by a Cryo-cooler. This simulates the Martian ambient conditions of 6.4mbar pressure and a temperature of 200K. Though the Martian atmosphere contains only 95.3% CO_2, presently the supply gas is composed entirely of CO_2.

2. The compressor, heat exchanger and heater form the CO_2 preparatory sub-system. In order to avoid a very bulky system at high CO_2 mass flow rates, the supply gas is pressurized from 6.4 mbar to higher pressures. At the present time CO_2 is assumed to be pressurized to 1bar. The reasons for this are two-fold. The Test Bed is operated on the Earth and operating the system at 1 bar minimises the probability of gas leaks. Secondly, electrochemical separation membranes have been tested extensively with other gases at 1 bar and higher pressures and its performance at lower pressures is not known currently. The effect of lower pressures on the electrochemical separation is the subject of a related investigation at UA/NASA SERC. After the compressor, the pressurized CO_2 enters a waste heat recovery heat exchanger to gain energy from the gases exhausting from a Zirconia (ZrO_2) Cell, which will be discussed later. The CO_2 supply gas then enters a heater where it reaches the same temperature as the ZrO_2 electrochemical separation membrane unit. Thermal decomposition of CO_2 occurs in the heater. Since the temperature of the gases entering the separation unit is the same as that of the unit itself, the separation unit is not subjected to any thermal shocks.

3. The mixture of CO, O_2 and CO_2 passes through the ZrO_2 cell, which electrochemically

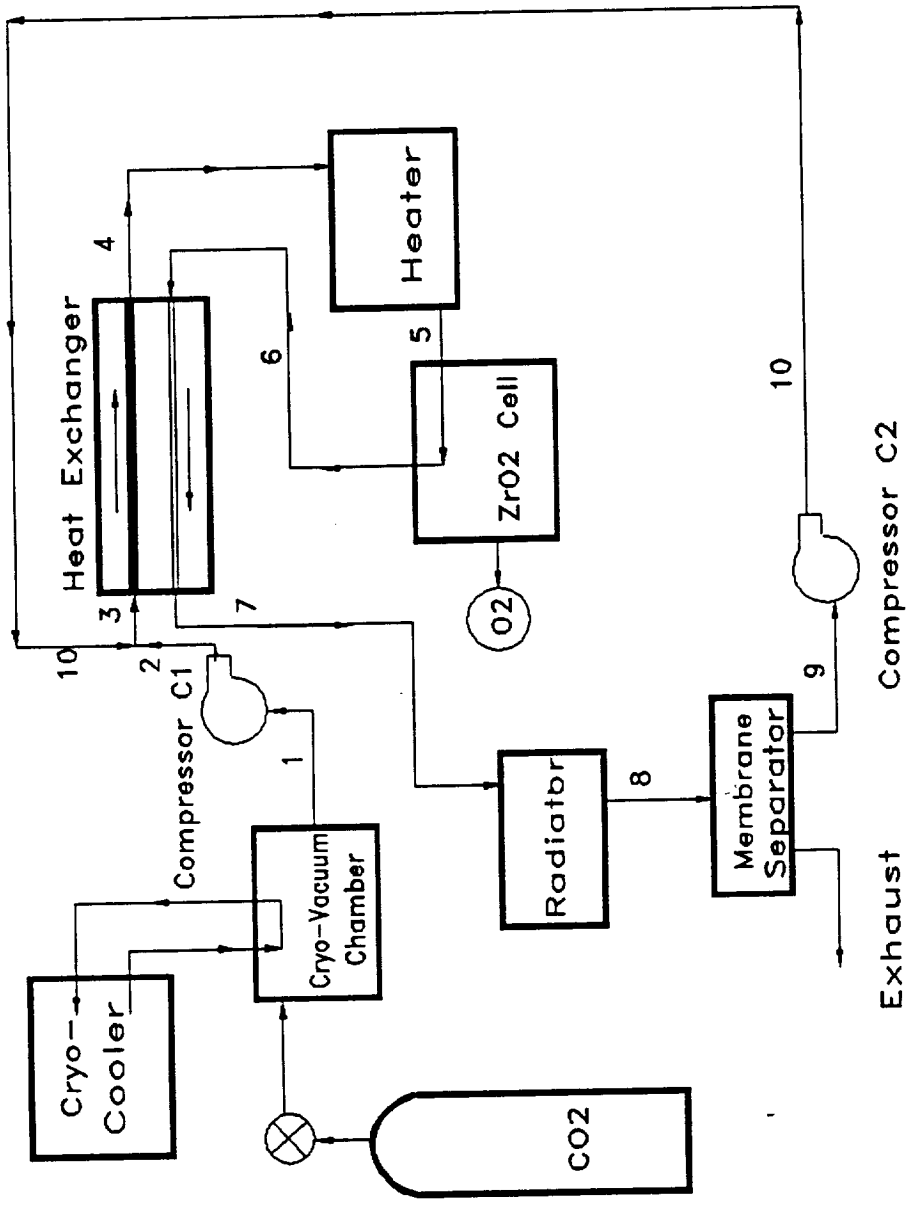

Fig 1: Test Bed With Recycling of Carbon Dioxide

separates the O_2 from the mixture. This O_2 is then fed to a storage device for later use. The cell forms the oxygen separation sub-system.

4. The exhaust from the Cell, after passing through the heat exchanger, loses energy in a radiator before passing through a polymeric membrane separator which separates the unreacted CO_2. The radiator is essential because polymeric membrane separators cannot withstand the high exhaust temperatures. There is a substantial pressure drop across the membrane separator, which requires a second compressor to re-pressurize the CO_2 to 1 bar. The CO_2 then re-enters the loop just before the heat exchanger. The system is depicted in figure 1.

Figure 2 illustrates the system without recirculation. The exhaust gas, after passing through the heat exchanger, is expelled from the system. Henceforth, the system with recycling is referred to as case 1, and the one without, as case 2. The number of moles of CO, CO_2 and O_2 flowing at various points in the system for both cases 1 and 2 is shown in table 1.

Nomenclature

e = Fraction of O_2 produced that is electrochemically separated by the cell.

μ_{sep} = Membrane Separation Factor = $\frac{\text{Amount of } CO_2 \text{ at Point 9}}{\text{Amount of } CO_2 \text{ at Point 8}}$

This is only for case 1.

α = Cell Factor ≡ moles of unreacted CO_2 for each mole of O_2 produced

This determines the cell efficiency τ_{cell} as:

$$\tau_{cell} = \frac{\text{moles of } O_2 \text{ actually produced}}{\text{theoretical max. no. of moles of } O_2 \text{ possible}} = 2/(2+\alpha)$$

The Cell reaction is:

$$[(2+\alpha)/e]CO_2 = [2/e]CO + [1/e]O_2 + [\alpha/e]CO_2$$

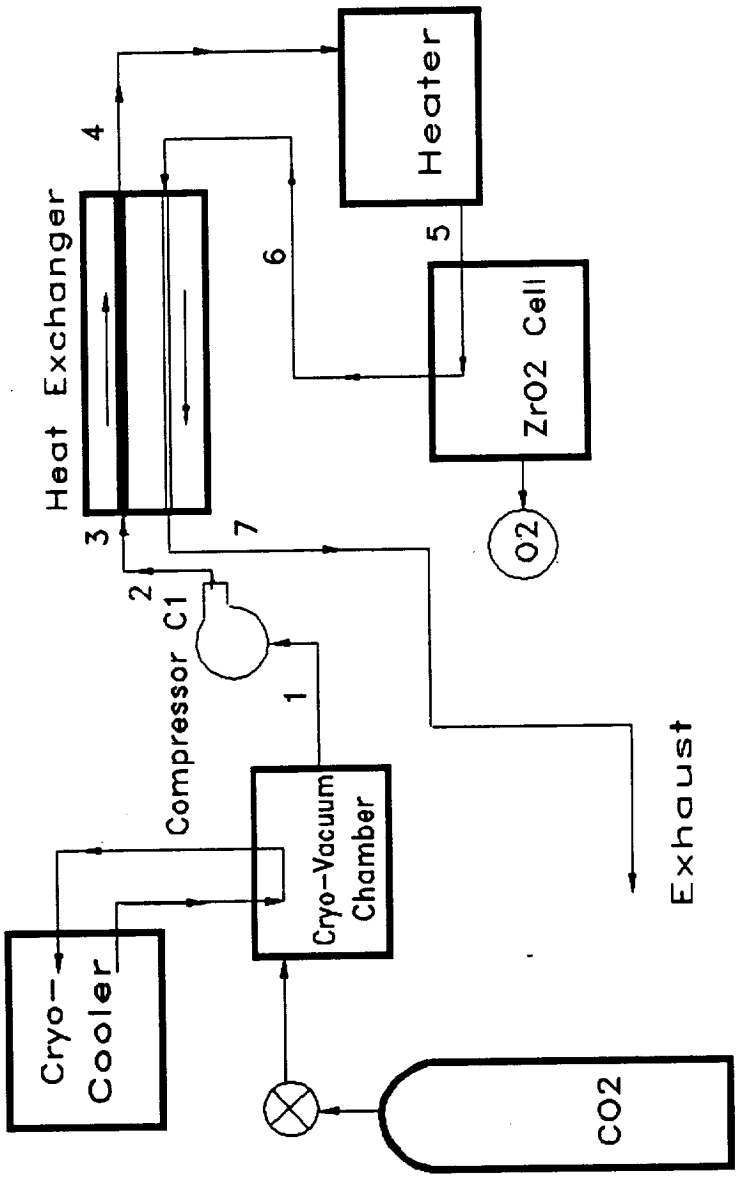

Fig 2: Test Bed Without Recycling of Carbon Dioxide

Table 1: For Oxygen Production of 1 mole

Point	Case 1	Case 2
1	$\frac{(2+\alpha-\mu_{sep}\alpha)}{\epsilon}CO_2$	$\frac{(2+\alpha)}{\epsilon}CO_2$
2	$\frac{(2+\alpha)}{\epsilon}CO_2$	$\frac{(2+\alpha)}{\epsilon}CO_2$
3	$\frac{(2+\alpha)}{\epsilon}CO_2$	$\frac{(2+\alpha)}{\epsilon}CO_2$
4	$\frac{(2+\alpha)}{\epsilon}CO_2$	$\frac{(2+\alpha)}{\epsilon}CO_2$
5	$\frac{(2+\alpha)}{\epsilon}CO_2$	$\frac{(2+\alpha)}{\epsilon}CO_2$
6	$[2/\epsilon]CO+[(1-\epsilon)/\epsilon]O_2+[\alpha/\epsilon]CO_2$	$[2/\epsilon]CO+[(1-\epsilon)/\epsilon]O_2+[\alpha/\epsilon]CO_2$
7	$[2/\epsilon]CO+[(1-\epsilon)/\epsilon]O_2+[\alpha/\epsilon]CO_2$	$[2/\epsilon]CO+[(1-\epsilon)/\epsilon]O_2+[\alpha/\epsilon]CO_2$
8	$[2/\epsilon]CO+[(1-\epsilon)/\epsilon]O_2+[\alpha/\epsilon]CO_2$	
9	$[\mu_{sep}\alpha/\epsilon]CO_2$	
10	$[\mu_{sep}\alpha/\epsilon]CO_2$	

Assumptions

The thermodynamic analysis has been performed based on the following assumptions:

1. The Membrane Separator filters out all the CO and O_2 from the exhaust gases. It is known that the purity of the separated gases is very high. Hence this is a valid first-order approximation.

2. Only a steady state analysis has been performed.

3. Pressure drop and heat losses in the pipes, valves and bends are negligible.

4. The Compressors have been assumed to be isentropic, with specified mechanical and isentropic efficiencies. Radiation losses from their surfaces have been neglected since they are small in comparison.

The analysis gives the total heat transferred from the exhaust to the fresh CO_2. Using an iterative procedure, the cold side outlet temperature and the Logarithmic Mean Temperature Difference (LMTD) are determined. Knowing the mass flow rates, the heat exchanger can be designed. The power requirement of the ZrO_2 cell - the Nernst potential and the ionic component of the current

corresponding to the oxygen ion flow can be calculated precisely. For a fixed O_2 production rate, it is a constant.

Discussion of Results

The analysis was performed with the help of an interactive program written in Pascal. The program has pull-down menus using which the user can change any of the input variables. This was necessary because the optimal cell temperature, cell efficiency and membrane separation factor is presently not known. Concurrent research is being done at UA/NASA SERC to investigate the optimum system performance conditions. Some graphs have been obtained from the data generated by using the program for an oxygen production rate of 10 kg/day, which corresponds to the production rate needed for an unmanned sample return mission [2]. Figure 3 shows the variation of the specific heats of CO_2, CO and O_2 with temperature. Empirical relationships [3] have been used to determine these curves. This variation in the specific heat (C_p) precludes treating C_p as a constant, say, across the heat exchanger. Over the entire range of temperatures considered, it is seen that C_p increases with temperature for all three gases, with the curve for CO_2 increasing most sharply. Figure 4 shows the graph of heater power with cell temperature (T_5). The power consumed by the heater increases with T_5 as expected, for low values of T_5. It reaches a maximum, and then, contrary to expectations, starts dropping. Figures 6 and 7 show plots of temperature of the cell (T_5) with the outlet temperature T_4 of the cold CO_2 from the heat exchanger. Though not apparent from the figures, (T_5-T_4) actually increases with T_5. The anomalous behaviour of figure 4 can be explained by the fact that though C_p itself increases, and (T_5-T_4) also increases, the integral of $C_p dT$ over the temperature range

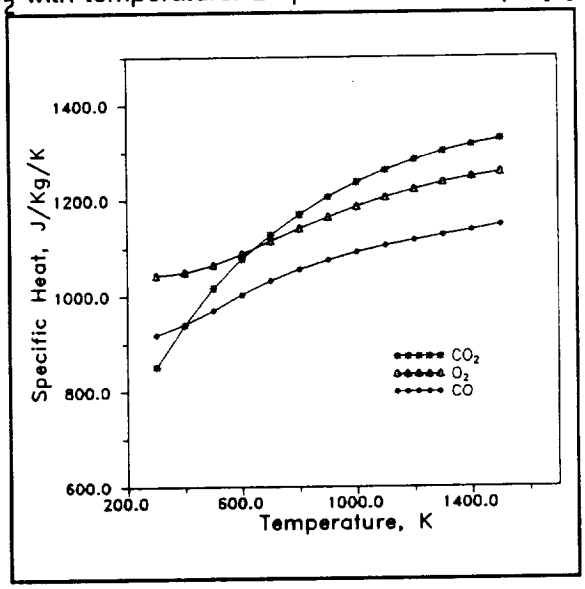

Fig 3: Variation in C_p

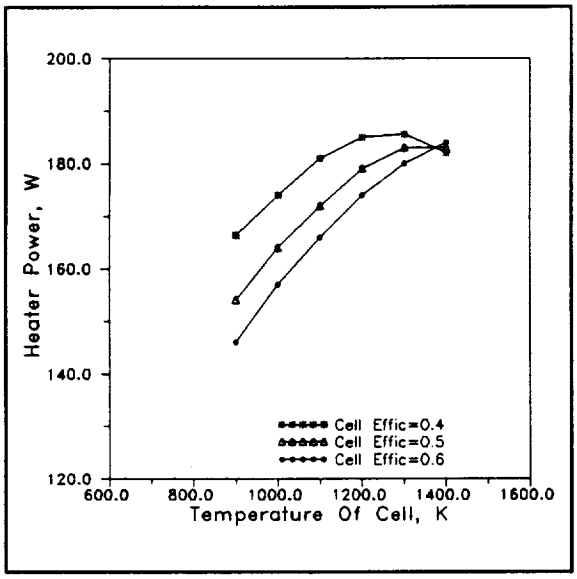

Fig 4: Heater Power - Case 1

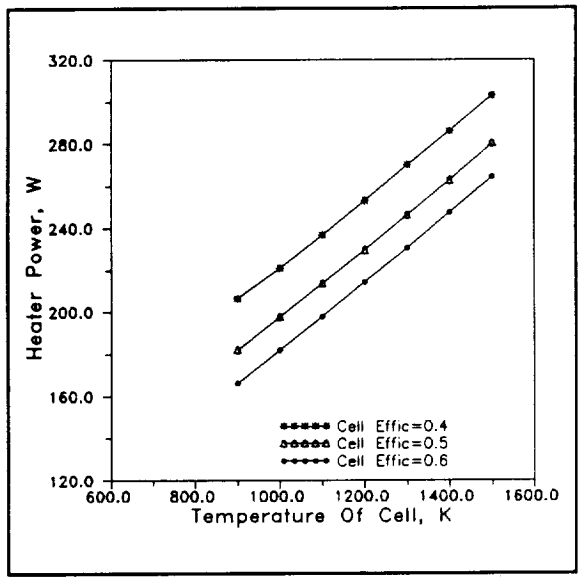

Fig 5: Heater Power - Case 2

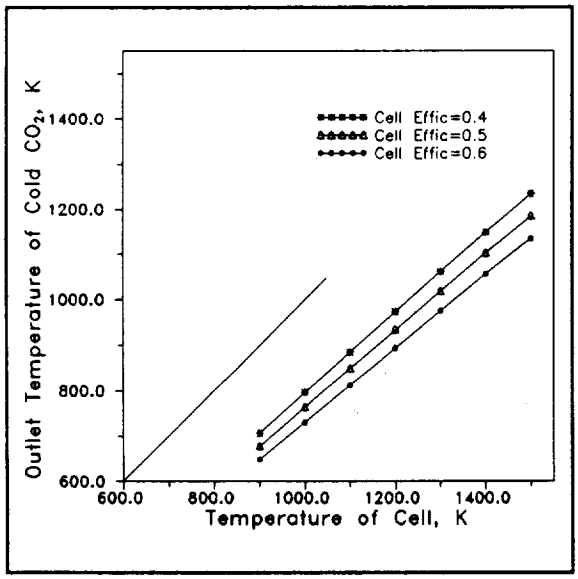

Fig 6: T_4 v/s T_5 - Case 1

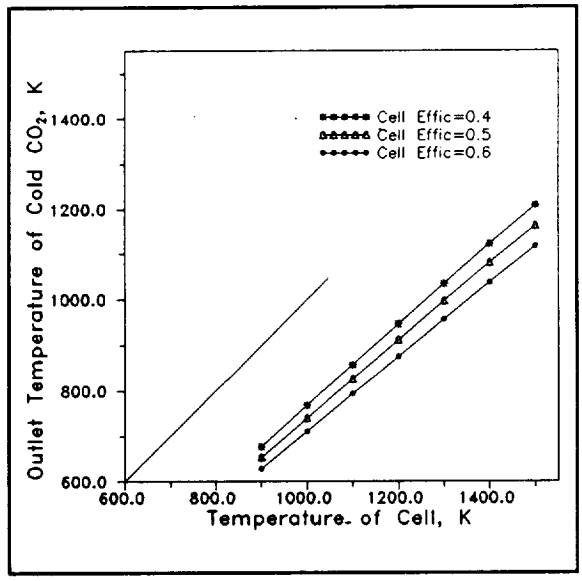

Fig 7: T_4 v/s T_5 - Case 2

T_4 to T_5 actually decreases after a point. This is opposed to the almost linear increase of heater power with temperature in case 2 as shown in figure 5. In this case, though the mass flow rates of CO_2 at points 4 and 5 are the same as in case 1, T_3, and hence T_4, are lower for the same value of T_5. This is because the recirculating CO_2 is at a higher temperature than that of the CO_2 at point 2. Hence, the increased (T_5-T_4) term counters the decrease in the slope of the C_p curve

enough to cause the heater work to increase. Here, and in discussions later in this report, we freely use the "(T_5-T_4)" argument. Although the empirical relations used for C_p were fourth-order polynomials in temperature, terms such as $(T_5^4-T_4^4)$ etc. depend essentially on (T_5-T_4). Note that the magnitude of heater work is greater for case 2 than for case 1, for a fixed T_5. It may be expected that at cell temperatures higher than those considered, figure 5 behave similar to figure 4. However, in practice, cell temperatures higher than 1500K are not of interest.

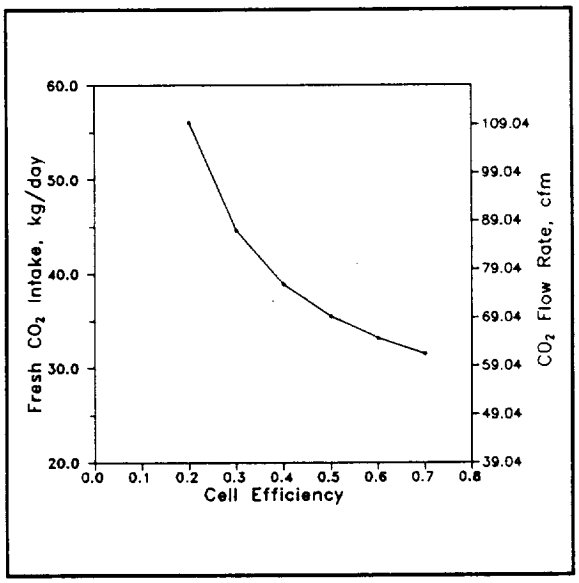

Fig 8: CO_2 Intake - Case 1

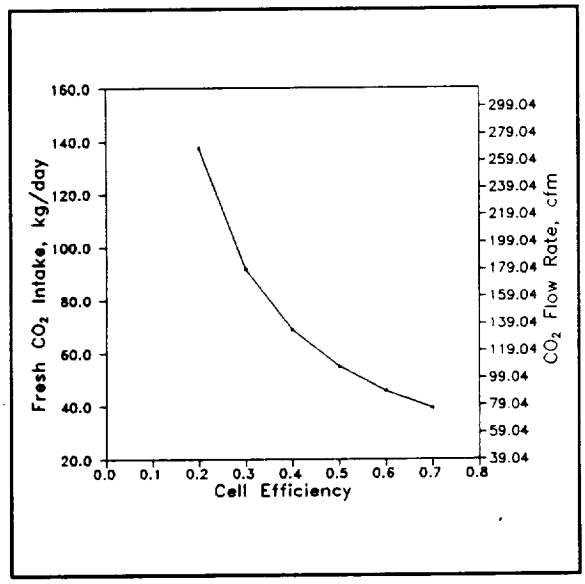

Fig 9: CO_2 Intake - Case 2

Figures 8 and 9 show the CO_2 intake required for cases 1 and 2 respectively. Clearly, the intake required increases sharply as the cell efficiency approaches zero. The intake in cubic-feet per minute (cfm) at the inlet pressure of 6.4 mbar gives us an idea of the size of pumps that we will require. Note that for a given cell efficiency, the intake required in case 2 is greater than that in case 1, especially at lower efficiencies. Since the slope of the curve decreases rapidly with increasing efficiency, and keeping in mind that the intake determines the capacity of the Compressor C_1, the conclusion is that the compressor capacity becomes impractical at very low efficiencies. For a start, we take an efficiency of 0.2 which is reasonable at this point of time. The pumping speed required is about 280 cfm for case 2 and about 115 cfm for case 1. If we take an

off-the-shelf vacuum pump which can fulfil these requirements, then for case 2, an S Series Rotary Vane Pump Model S630F manufactured by Leybold Vacuum Products Inc. will suffice. It weighs 1450 lb and has a power requirement of 25 hp. For case 1, where the CO_2 is recycled, a much smaller pump such as the Leybold Model S160C, which weighs 310 lb and consumes 7.5 hp can do the job. Also required in case 1 is a much smaller pump (compressor C_2) to compensate for the pressure drop across the membrane separator. For this a small pump like the Leybold TRIVAC Rotary Vane Pump Model D2A will do. This pump weighs 41 lb and consumes 0.33 hp. This clearly indicates that at this point, though case 2 appears compelling from the points-of-view of system simplicity and reliability, we must recycle the CO_2 in order to design a reasonably compact system. Note that we must also consider the mass added to the system by the radiator and the membrane separator. However, the reduction in compressor mass and power obtained by recycling offsets the increase in mass due to the radiator and membrane separator. Having decided on recycling, we take an optimistic look at what our requirements would be if we were successful in obtaining a cell efficiency of, say, 0.5, which gives us a CO_2 intake of about 70 cfm. To take care of this requirement, a first approximation would be a pump like the Leybold S100C, with a mass of 220 lb and a power requirement of 5.0 hp. This makes the system design very feasible as far as its mass requirements go. Obviously, for an actual mission, a much more

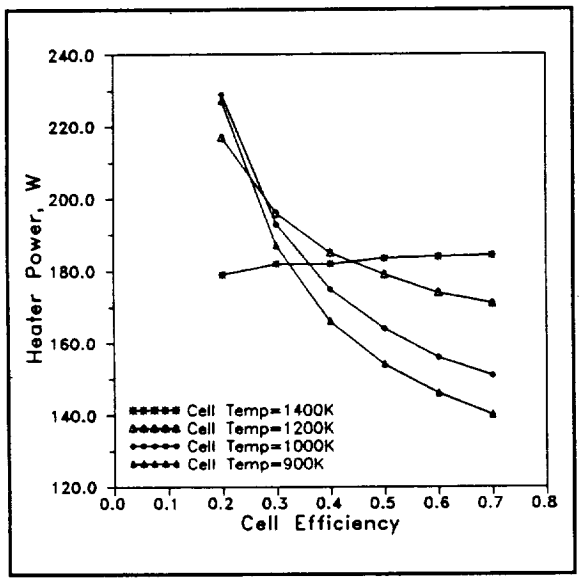

Fig 10: Heater Power v/s τ_{cell} - Case 1

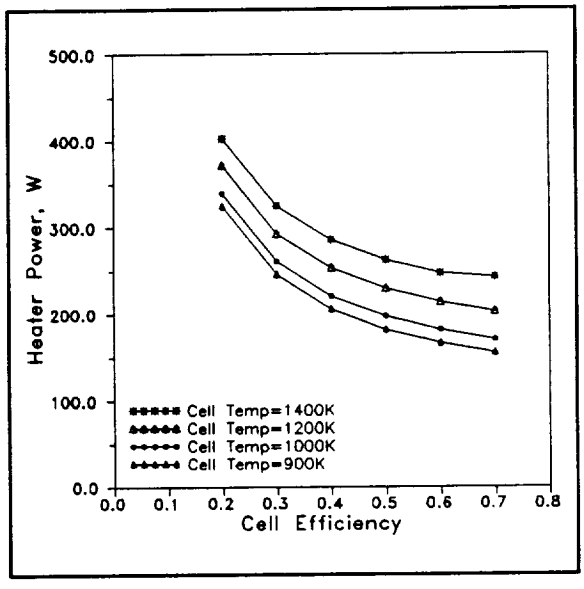

Fig 11: Heater Power v/s τ_{cell} - Case 2

sophisticated pump with better materials and design would be used. But it would depend on whether an efficient Zirconia cell can be designed. Figure 10 is a graph of heater power versus cell efficiency for case 1. In the light of information obtained from figures 4 and 10, we realise that at low efficiencies the heater power increases because of increased CO_2 mass flow rate. But the interesting point made by this graph is that at higher cell temperatures and lower efficiencies, the effect of the cell temperature prevails, and causes the slope of the curve to decrease.In fact, the curve for a cell temperature of 1400K is almost flat, suggesting that there could be a temperature T_5 between 1400K and 1200K at which the load on the heater is almost constant. Also important is the fact that it is a lower temperature difference (T_5-T_4) that "overcomes" the increase in the slope. Figure 11, for case 2, is clearly a follow-up of figure 5. Here, the temperature difference (T_5-T_4) does not fall sufficiently to cause the slope to decrease.

Plans For The Future

1. The system design depends, to a large extent, upon the system operating pressure. The optimum system pressure needs to be examined. If the system pressure were low, then the option of using a blower (lower mass) instead of a compressor will be examined.

2. The heat exchanger design presently limits the exhaust gas temperature to 700K, due to fears of carbon deposition. Suitable changes will be made in the design when a related investigation by Prof. D.C. Lynch, Department of Materials Science, University of Arizona, provides results on the seriousness of carbon deposition.

3. The pressure and heat losses in the system components and piping will be incorporated in the analysis and

4. The individual components will be designed and tested.

Acknowledgements

The graphics routines of the Pascal program used in the analysis were written by Mario Rascon and Kirby Hnat. Their help is gratefully acknowledged.

References

1. K. Ramohalli, E. Lawton & R. Ash, "Recent Concepts in Missions to Mars: Extraterrestrial Processes", Journal of Propulsion and Power, Vol 5, pp 181-187, 1989

2. R.L. Ash, W.L. Dowler & G. Varsi, " Feasibility of Rocket Propellant Production on Mars", Acta Astronautica, Vol 5, pp 705-724, 1978

3. Thermophysical Properties of Matter, The TPRC Data Series, Vol 6, p 50, 145 & 154, IFI/Plenum, 1970